Sodium–Alanine Cotransport in Renal Proximal Tubule Cells Investigated by Whole-Cell Current Recording

JOACHIM HOYER and HEINZ GÖGELEIN

From the Max-Planck-Institut für Biophysik, D-6000 Frankfurt a.M. 70, Germany

ABSTRACT Sodium–alanine cotransport was investigated in single isolated proximal tubule cells from rabbit kidney with the whole-cell current recording technique. Addition of L-alanine at the extracellular side induced an inward-directed sodium current and a cell depolarization. The sodium–alanine cotransport current was stereospecific and sodium dependent. Competition experiments suggested a common cotransport system for L-alanine and L-phenylalanine. Sodium–alanine cotransport current followed simple Michaelis-Menten kinetics, with an apparent K_m of 6.6 mM alanine and 11.6 mM sodium and a maximal cotransport current of 0.98 pA/pF at −60 mV clamp potential. Hill plots of cotransport current suggested a potential-independent coupling ratio of one sodium and one alanine. The apparent K_m for sodium and the maximal cotransport current were potential dependent, whereas the apparent K_m for L-alanine was not affected by transmembrane potential. The increase in K_m for alanine with decreasing inward-directed sodium gradients suggested a simultaneous transport mechanism. These results are consistent with a cotransport model with potential-dependent binding or unbinding of sodium (high-field access channel) and a potential-dependent translocation step.

INTRODUCTION

In the renal proximal convoluted tubule a major fraction of the glomerularly filtered solutes are reabsorbed. Similar to numerous solutes like glucose, lactate, and phosphate, the uptake of neutral amino acids from the tubule lumen into the cell is mediated by sodium-substrate cotransport systems (for review see Ullrich, 1979; Schafer and Williams, 1985; Silbernagl, 1988). These secondary active transport processes are energized by the electrochemical sodium gradient, which is generated by the $(Na^+ + K^+)$-ATPase located in the contraluminal plasma membrane.

The sodium dependence of amino acid transport was shown by Fox et al. (1964) in renal cortical slices, as well as by Lingard et al. (1973) and Ullrich et al. (1974, 1976)

Address reprint requests to Dr. J. Hoyer, Universitätsklinikum Steglitz, Hindenburgdamm 30, D-1000 Berlin 45, Germany.

Dr. Hoyer's present address is Medizinische Klinik und Poliklinik, Universitätsklinikum Steglitz, Hindenburgdamm 30, 1000 Berlin 45, Germany. Dr. Gögelein's present address is Hoechst AG, Pharmaforschung, D-6230 Frankfurt/Main, Germany.

J. GEN. PHYSIOL. © The Rockefeller University Press · 0022-1295/91/05/1073/22 $2.00
Volume 97 May 1991 1073–1094

with in vivo microperfusion experiments. Studies using vesicles prepared from epithelial brush-border membranes (Sigrist-Nelson et al., 1975; Evers et al., 1976; Fass et al., 1977) also demonstrated the sodium dependence and electrogenicity of amino acid cotransport systems. Furthermore, the effect of membrane diffusion potentials on amino acid uptake (Evers et al., 1976; Burckhardt et al., 1980) and of sodium gradients on transport kinetics (Fass et al., 1977) were investigated, as well as the specificity of amino acid cotransport systems (Mircheff et al., 1982; Lynch and McGivan, 1987).

Several groups applying electrophysiological techniques in the proximal tubule (Burg et al., 1976; Hoshi, 1976; Samarzija and Frömter, 1975, 1982; Frömter, 1982) or in a kidney cell line (Schwegler et al., 1989) described the general characteristics and demonstrated the electrogenic character of cotransport. Frömter and co-workers have studied the sodium-coupled amino acid transport in proximal tubules with the in vivo micropuncture technique (Frömter, 1981, 1982; Samarzija and Frömter, 1982). These authors identified at least five distinct amino acid cotransport systems in the rat proximal tubule. Moreover, they analyzed cotransport kinetics and defined the driving forces acting on the cotransport mechanism: i.e., cell membrane potential, Na^+ ion gradient, and the substrate concentration gradient.

Though kinetic data on the sodium-coupled uptake of amino acids into the proximal tubule cells have been provided (Evers et al., 1976; Ullrich et al., 1976; Fass et al., 1977; Samarzija and Frömter, 1982; Lynch and McGivan, 1987), little is known about the mechanism of the cotransport and the effect of the transmembrane potential on cotransport kinetics and transport mechanism.

In the present study the cotransport of Na^+ ions and L-alanine in isolated proximal tubule cells was investigated with the tight-seal, whole-cell recording method as described by Marty and Neher (1983), measuring the whole-cell current induced by the cotransport. This technique allows one to control all three driving forces acting on the cotransport, (*a*) by clamping the cell to any distinct membrane potential and (*b*) by perfusing the cell with the pipette solution and therefore controlling the substrate gradients. Jauch et al. (1986) applied the tight-seal whole-cell current recording technique especially to investigate the effects of membrane potentials on sodium-alanine cotransport in pancreatic acinar cells. They characterized kinetic properties of the cotransport system and performed a theoretical treatment, yielding a model with a simultaneous transport mechanism (Läuger and Jauch, 1986).

In this study, after some basic characterization of the sodium–alanine cotransport in the isolated proximal tubule cells, we investigated the cotransport kinetics and its dependence on transmembrane potential. The kinetic analysis yielded information on the transport mechanism and the influence of the cell potential on the cotransport properties.

Parts of this study were presented at the 75th conference of the Deutsche Gesellschaft für Biologische Chemie (1989. *Biol. Chem. Hoppe-Seyler.* 370:623).

METHODS

Cell Isolation

The cell isolation procedure was adopted from methods described by Heidrich and Dew (1977) and Poujeol and Vandewalle (1985), avoiding the use of chelating agents or proteolytic

treatment. Proximal tubule cells were isolated from kidneys from New Zealand White rabbits. Rabbits weighing 800–1,200 g were killed by cervical dislocation and exsanguinated. The kidneys were rapidly excised and placed in ice-cold isolation buffer containing (in mM): 150 K-cylamate, 10 HEPES, 1 $Cacl_2$, and 1 $MgCl_2$, pH 7.4. The following steps were performed on ice: After decapsulation superficial cortical slices ~0.5 mm thick were dissected and minced with a scalpel. The tissue was homogenized in a Dounce homogenizer by three strokes with a loose-fitting pestle. The homogenate was then poured through graded sieves (250, 75, and 40 μm) to obtain a population of single cells. Cells were stored on ice until use. This isolation procedure yielded single proximal tubule cells within <30 min. Since the predominant tubule section of the cortex cortices of the rabbit kidney is the pars convoluta of the proximal tubule (Kaissling and Kriz, 1979) it can be concluded that the majority of the isolated cells in the cell suspension were of proximal tubule origin. By light microscopy cells were identified by long microvilli distributed over the entire cell surface and could easily be discriminated from remaining erythrocytes, cell detritus, and tubulus fragments under the microscope. Cell viability was verified by Trypan blue exclusion.

Electrical Measurements

For patch clamp experiments cells were transferred into a measuring chamber mounted on the stage of an inverted microscope (magnification × 400, IM 35; Zeiss, Oberkochen, Germany). Most experiments were performed at room temperature.

Patch clamp data recording and analysis were in general similar to those described in previous reports (Hamill et al., 1981; Gögelein and Greger, 1987). Patch pipettes were manufactured from borosilicate glass capillaries (Science Product Trading, Frankfurt a.M., Germany) of 0.3 mm wall thickness and firepolished as described by Hamill et al. (1981). Pipettes routinely had resistances of 3–6 MΩ measured in 140 mM NaCl solution. Whole-cell currents were recorded with a patch clamp amplifier (L/M EPC 7; List Electronic, Darmstadt, Germany), which was connected to a remote control unit (Rohlicek et al., 1989). Current and voltage signals were stored on VHS videotape with a conventional video recorder (VT-315; Blaupunkt, Hildesheim, Germany) after being digitized with a pulse-code modulator (PCM 501; Sony, Köln, Germany). As described by Bezanilla (1985), the bandwidth of the PCM 501 was extended to direct current and low-pass filters with Butterworth characteristics were replaced by filters with Bessel characteristics (4-pole, 9-kHz bandwidth; our own workshop).

The data were analyzed off-line with a computer system (LSI 11/23; Digital Equipment Corp., Marlboro, MA). After low-pass filtering with a 4-pole Bessel filter (−3 dB at 0.4 kHz), data were sampled with a sample time of 1 ms. The patch clamp preamplifier was mounted on a micromanipulator (our own workshop) consisting of micrometer plates driven by remote-controlled electrical motors (for fast positioning of the patch pipette) in combination with piezo elements (for fine movements of a few micrometers). After the pipette was gently pushed against the cell membrane, a gigaseal was established by applying slight suction on the pipette interior. The whole-cell configuration was established by breaking the membrane patch under the patch pipette with short pulses of suction. Immediately afterward the cell potential was measured in the current-clamp mode (CC) of the EPC 7 amplifier. The cell capacity was determined with the slow capacitance cancellation network of the EPC 7 amplifier. In some experiments cell capacity (C) and series resistance (R_s) were also determined from amplitude (δI) and time constant (τ) of the transient current, induced by a voltage step command of amplitude δV, according to $R_s = \delta V/\delta I$ and $C = \tau/R_s$. For this purpose whole-cell current signals had to be filtered with 20–30 kHz and were displayed on a digital oscilloscope. Cell capacities calculated with this method correlated well with the values determined by the EPC-7 cancellation network.

Measurement of the current–voltage relationship was usually performed within a clamp

potential range from −80 to +80 mV, measuring whole-cell currents induced by short voltage pulses (300 ms) in 20-mV steps of alternating polarity.

After the whole-cell configuration had been established, the pipette together with the cell could cautiously be lifted from the bottom of the bath without disturbing electrical properties. To perform solution exchanges on the extracellular side, a pipette system consisting of up to eight glass pipettes (0.1 mm i. d., arranged in parallel) was placed in the bath. Each pipette was prefilled with a test solution. For solution exchange the cell was moved into the respective pipette (~100–200 μm). A modified perfusor (Perfusor ED 2; Braun, Melsungen, Germany), pumping the test solutions with a flow rate of 15–20 μl/min, guaranteed that the cell was always completely surrounded with the respective pipette solution. This set-up allowed the exchange of the extracellular solution within seconds without destroying the tight-seal between patch pipette and cell membrane. Unless indicated otherwise, the pipette solution contained (in mM): 140 Na-cyclamate, 40 D-mannitol, 10 HEPES, 1 $MgCl_2$, 1 EGTA, and 0.73 $CaCl_2$, yielding a free calcium concentration of 10^{-7} M, pH 7.2. The bath solution contained (in mM): 140 Na-cyclamate, 10 HEPES, 1.3 $CaCl_2$, 1 $MgCl_2$, pH 7.4, and 0–40 L-alanine; osmolarity was balanced with D-mannitol. Therefore, standard experiments were performed with symmetrical ion concentrations, vanishing intracellular amino acid concentration, and in the absence or presence of extracellular amino acids. In some experiments the intracellular solution contained Tris instead of sodium. In the latter cases, whole-cell current data were corrected for the resulting voltage offset.

The sign of the clamp potential refers to the cell interior with respect to the extracellular or bath side. Whole-cell currents carried by cations moving from the bath into the cell are depicted as negative currents. The reference electrode consisted of a chloridized silver wire connected via an agar bridge (50 g/liter agar in 140 mM NaCl) to the bath solution. An Ag/AgCl electrode was also used in the patch pipette. Therefore, only the lower part of the patch pipette was filled with cyclamate solutions (see above), while the upper part, surrounding the chloridized silver wire, was filled with a 140 mM NaCl solution.

The subscript i denotes the intracellular or pipette solution, respectively, and the subscript o denotes the extracellular or bath solution, respectively. The whole-cell current could be measured with an accuracy of ~0.2 pA. All values are given as means ± SEM. All chemicals were of analytical grade.

RESULTS

Basic Observations

Electrical parameters of the whole-cell current recordings are shown in Table I. The series resistance was in the order of two magnitudes smaller than the membrane resistance, thus having a negligible impact on current measurements. Cell capacity is a good measure for the cell membrane area (A), assuming a specific membrane capacity of $C_m/A = 1\ \mu F/cm^2$. In our experiments cell capacity correlated well with the alanine-driven sodium current (data not shown). Therefore, cell capacity was used for standardization of whole-cell currents from different experiments. From 17 experiments a mean cell capacity of 8.0 ± 1.1 pF for single cells was calculated.

Immediately after the whole-cell configuration was established, large fluctuating positive currents, presumably representing an efflux of positive ions (potassium) from the cell, and negative cell potentials in the range of −15 to −70 mV were observed. Both positive currents and negative cell potentials diminished to 0 ± 0.5 pA and 0 ± 5 mV, respectively, within 15–30 s, indicating an efficient dialysis of cells with the pipette solution.

L-Alanine-Driven Whole-Cell Current

An original recording of whole-cell currents and clamp potentials in the absence (control) and presence of 20 mM L-alanine is shown in Fig. 1 *A*. Under symmetrical sodium concentrations ($[Na^+]_i = [Na^+]_o = 140$ mM) the whole-cell current at 0 mV clamp potential was ~0 pA. The addition of 20 mM L-alanine to the bath at 0 mV clamp potential resulted in a negative whole-cell current representing an influx of positively charged sodium ions driven by L-alanine.

When experiments were performed in single cells, the alanine-driven sodium current could be sustained for several minutes at the initial current level, yielding 2.5 ± 0.5 pA at 0 mV and 20 mM L-alanine ($n = 16$). In contrast, the alanine-driven sodium current declined with time, when measurements were performed in cell clusters (four to six cells), indicating a delayed or ineffective dialysis of coupled cells. Therefore we preferred to experiment with single cells. The effect of L-alanine was reversible and could be repeated several times within one experiment.

TABLE I

Whole-Cell Recording Parameters

Pipette resistance	3–8 MΩ
Series resistance	20–40 MΩ
Seal resistance	10–80 GΩ
Membrane resistance	2–25 GΩ
Membrane capacity	3–40 pF

Tight-seal, whole-cell recording parameters. Pipette resistance was measured before touching the cell in symmetrical pipette and bath solutions: 140 mM NaCl, 10 mM HEPES, 1.3 mM $CaCl_2$, 1 mM $MgCl_2$, pH 7.4. Series resistance was measured after seal formation in the cell-attached mode and before membrane rupture. Membrane resistance was measured after breaking membrane patch under patch pipette under control conditions. Membrane capacity was determined with the slow capacitance cancellation network of a List EPC-7 patch clamp amplifier. Values of membrane capacity are from experiments with single cells or small cell clusters of two or three cells.

The whole-cell current traces recorded in response to different clamp potentials are illustrated with an extended time scale in Fig. 1 *B*. The effect of L-alanine on the whole-cell current is more pronounced at negative clamp potentials and diminishes with increasing positive clamp potentials.

In Fig. 1 *C* the corresponding *I-V* curves are shown. Under control conditions the *I-V* curve was linear in the potential range of ±60 mV and symmetrical to 0 mV. After addition of L-alanine to the bath, the current was shifted to more negative values. The alanine-driven, inward-directed sodium current is obtained by the difference between both curves. The two curves could be approximated by linear regression. In the presence of 20 mM L-alanine the intercept of the curve with the *x* axis was shifted to a positive potential of +19.5 mV (+22.4 ± 1.9 mV; $n = 14$). This potential resembles cell depolarization induced by the sodium–alanine cotransport into the cell, as observed by microelectrode analysis (Samarzija and Frömter, 1975, 1982; Hoshi, 1976). 10 mM L-alanine induced a depolarization of +13.2 ± 1.1 mV ($n = 4$) and with high L-alanine concentrations (40 mM) cells were depolarized by about +30 mV.

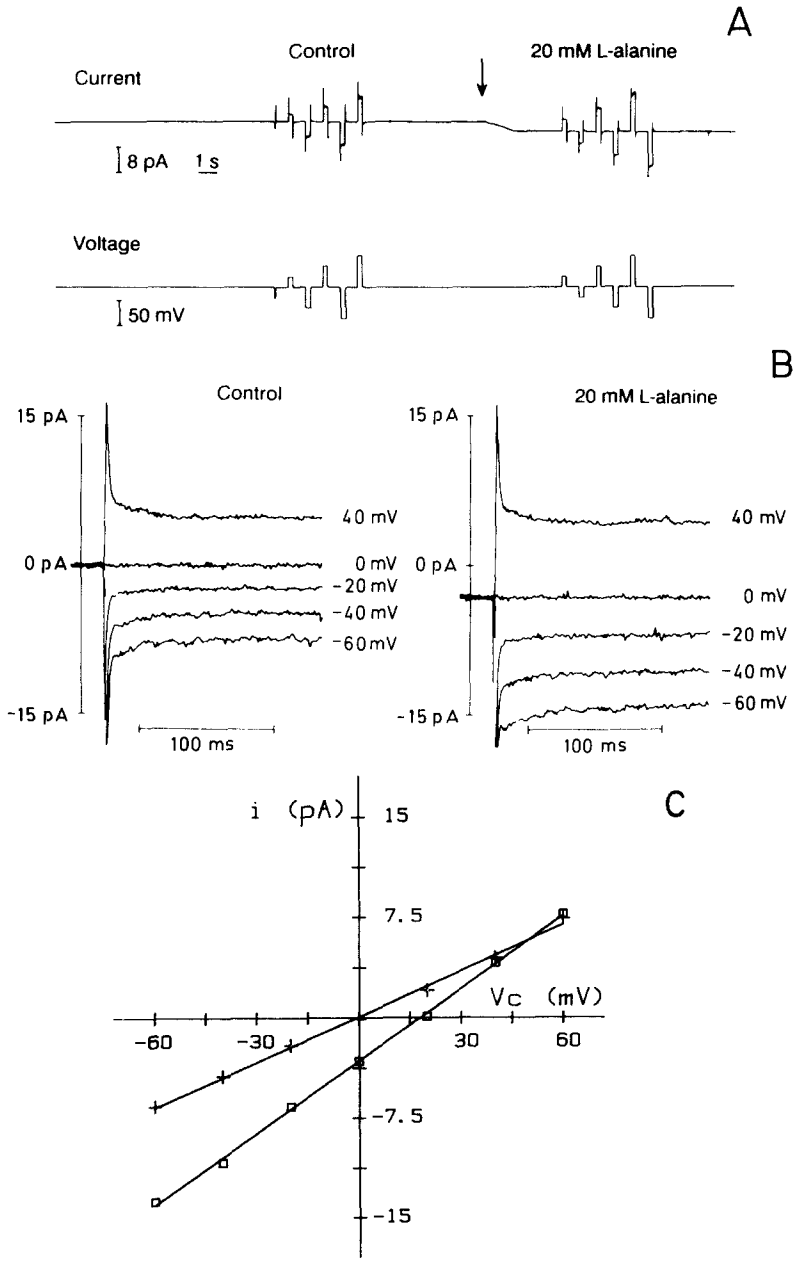

FIGURE 1. Alanine-driven inward-directed sodium current recorded in single proximal tubule cells under voltage clamp conditions. (*A*) Original recording trace of whole-cell current (*upper trace*) and clamp potential (*lower trace*) in the absence (*control*) and presence of 20 mM L-alanine. Under control conditions both the pipette and external solutions were alanine-free. Pipette solution: 140 mM Na-cyclamate, 0.73 mM $CaCl_2$, 1 mM EGTA, 40 mM D-mannitol, pH 7.2. External solution: 140 mM Na-cyclamate, 1.3 mM $CaCl_2$, 40 D-mannitol, pH 7.4). Arrow indicates addition of 20 mM L-alanine to the bath solution. Under control conditions as well as

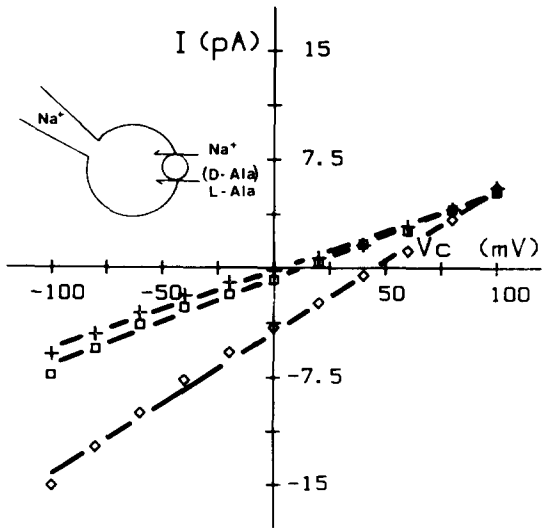

FIGURE 2. Current–voltage relation in the absence (+) and presence of 40 mM of either the L- (◇) or D-isomer (□) of alanine. Pipette solution: 140 mM Na-cyclamate, 0.73 mM $CaCl_2$, 1 mM EGTA, 40 mM D-mannitol, pH 7.2. External solution: 140 mM Na-cyclamate, 1.3 mM $CaCl_2$, 0 or 40 D- or L-alanine, 0 or 40 D-mannitol, pH 7.4. Cell capacity was 8.5 pF. Experiment was performed at room temperature.

General Properties of Sodium–Alanine Cotransport

In this section we describe experiments concerning the sterospecificity and sodium and temperature dependence. Fig. 2 demonstrates that the naturally occurring L-isomer of alanine induced a five to six times greater inward-directed whole-cell current than the same concentration of D-alanine. This sterospecificity was proven in four separate experiments. In experiments where extracellular sodium was replaced by potassium or Tris (data not shown), no effect of L-alanine on the whole-cell current was detectable, illustrating the requirement of this cotransport system for sodium in proximal tubule cells.

Because of the fragility of the isolated cells at temperatures >25°C, experiments in general were performed at room temperature. Only in a few experiments was it possible to measure the alanine-driven sodium current as a function of temperature. This current strongly increased with temperature and a Q_{10} value of 2.95 (±0.29; $n = 3$) could be calculated. From the Arrhenius equation ($d\ln I/d[1/T] = -E_a/R$) an activation energy of $E_a = 83$ J/mol was determined.

---

after addition of L-alanine, whole-cell currents were recorded in response to short voltage pulses (300 ms), alternating into positive and negative voltage direction. (*B*) Whole-cell currents recorded in response to different clamp potentials under control and after addition of L-alanine are superimposed and presented at an extended time scale. (*C*) Current–voltage relation under control conditions (+) and after addition of 20 mM L-alanine (□) to the external solution. Difference between the two curves reflects the alanine-driven inward-directed sodium current. The shift of the *x* axis intercept to a positive potential reflects the depolarization of the cell by the sodium–alanine cotransport. Cell capacity was 6.0 pF. Experiment was performed at room temperature.

Varying alanine gradient, no sodium gradient. In Fig. 3 *A* an original current trace measured at 0 mV clamp potential and varying alanine concentrations on the extracellular side is displayed. This figure and the I-V curves of the same experiment (Fig. 3 *B*) show that the cotransport is concentration dependent at low substrate concentrations and saturates at high $[\text{alanine}]_o$. The shape of the respective current–concentration curves at 0 and −60 mV in the Michaelis-Menten plot (Fig. 3 *C*) is a hyperbole indicative of a Michaelis-Menten kinetic behavior of the sodium–alanine cotransport.

Fig. 4 *A* illustrates results from six experiments where the whole-cell current was recorded as a function of extracellular L-alanine concentration. The experiments were performed in the presence of increasing L-alanine gradients and in the absence of a sodium gradient ($[Na^+]_i = [Na^+]_o = 140$ mM). For kinetic analysis the data points are displayed in Hanes plots (Fig. 4 *B*). An apparent K_m (intercept with the x axis) of 19.5 ± 4.1 mM L-alanine at 0 mV and an apparent maximum current (1/slope) $I_{max} = 0.54 \pm 0.08$ pA/pF at 0 mV were obtained. In experiments performed at a clamp potential of −60 mV, similar to membrane potentials measured in micropuncture experiments in intact rabbit proximal tubules (Biagi et al., 1981; Lapointe et al., 1984), the apparent K_m was nearly unaltered (19.8 ± 6.2 mM) and the apparent I_{max} increased to 0.94 ± 0.11 pA/pF.

Varying alanine gradient, fixed sodium gradients. Measurements were performed where Tris replaced sodium in the pipette solution, so that an inward-directed sodium gradient was present, in addition to the inward-directed alanine gradient. The results from seven experiments are illustrated in Fig. 5 *A*. The corresponding Hanes plot (Fig. 5 *B*) yielded an apparent K_m of 7.8 ± 0.8 mM for L-alanine and an apparent I_{max} of 0.57 ± 0.04 pA/pF at 0 mV clamp potential. At a potential of −60 mV K_m decreased slightly to 7.1 ± 0.6 mM L-alanine, whereas I_{max} increased to 0.99 ± 0.06 pA/pF. Compared with the experiments performed with symmetrical sodium concentrations (Fig. 4) the inward-directed Na^+ gradient increased the apparent affinity for alanine from 19.5 to 7.8 mM without having an impact on the apparent maximum current of the cotransporter.

Fig. 6 *A* illustrates the results from experiments ($n = 4$), where the alanine-driven sodium current was measured as a function of extracellular alanine and with $[Na^+]_o =$ 30 mM and $[Na^+]_i = 0$ mM. Fig. 6, *B* and *C*, illustrate the change of the apparent K_m for alanine from 37.6 ± 3.0 to 22.5 ± 5.3 mM and of the apparent I_{max} from 0.48 ± 0.08 to 0.73 ± 0.11 pA/pF, respectively, induced by cell hyperpolarization from 0 to −60 mV.

Varying sodium gradient, fixed alanine gradient. Whole-cell currents were also measured as a function of the sodium gradient. These experiments ($n = 4$) were performed with increasing inward-directed sodium gradients and an L-alanine gradient of $[\text{L-alanine}]_o = 60$ mM versus $[\text{L-alanine}]_i = 0$ mM. The concentration dependence of the cotransport current again indicated Michaelis-Menten behavior (Fig. 7 *A*). The corresponding Hanes plot (Fig. 7 *B*) revealed an apparent K_m of 14.3 ± 2.6 mM for sodium and an apparent I_{max} of 0.62 ± 0.05 pA/pF at 0 mV. Cell

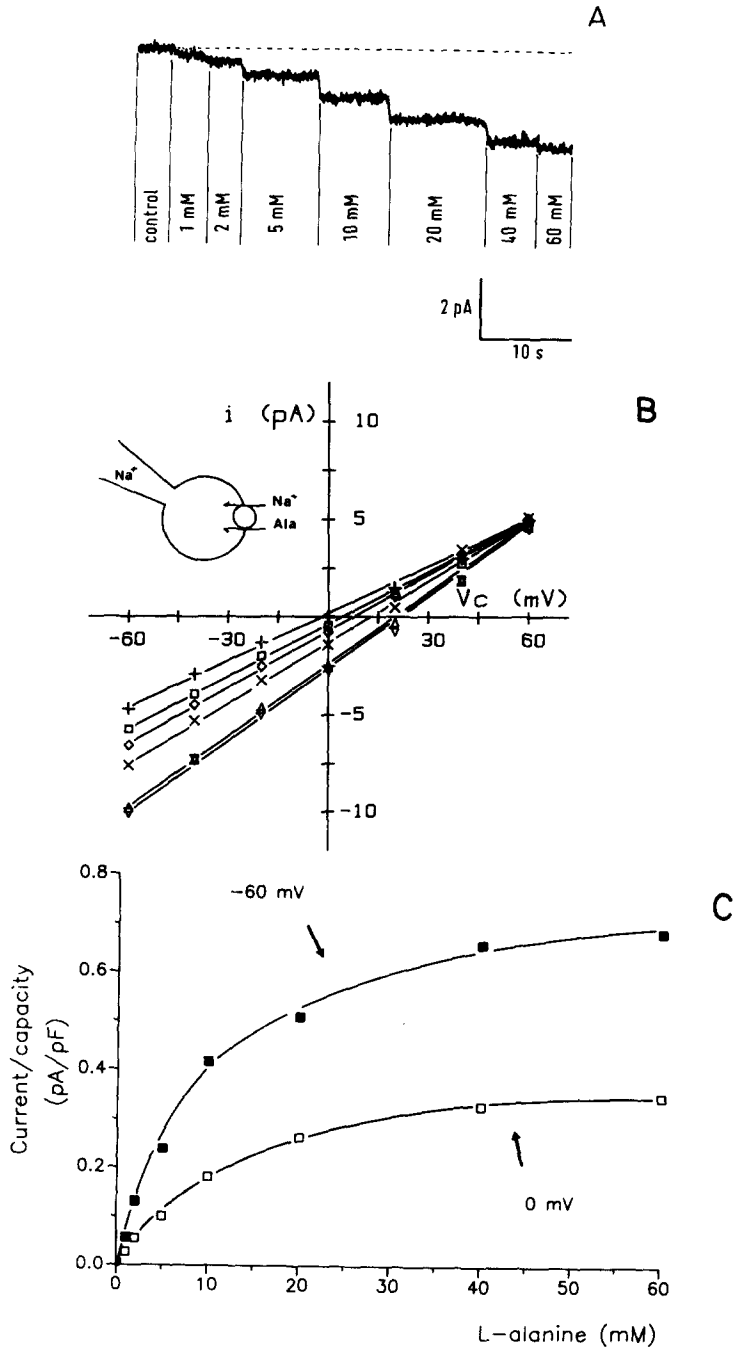

FIGURE 3. (*A*) Original current trace of a single PCT cell at V_c = 0 mV and increasing extracellular L-alanine concentrations. Pipette solution: 140 mM Na-cyclamate, 0.73 mM $CaCl_2$, 1 mM EGTA, 60 mM D-mannitol, pH 7.2. External solution: 140 mM Na-cyclamate, 1.3 mM $CaCl_2$, 0–60 mM D-mannitol, 0–60 mM L-alanine, pH 7.4. Cell capacity was 7.8 pF. The dashed line marks the current at 0 mM L-alanine (*control*). In *B* the respective *I-V* curves are shown at L-alanine concentrations of 2 (□), 5 (◇), 10 (×), 40 (△), and 60 mM (▽). *C* demonstrates the dependence of the whole-cell current on the L-alanine concentration at clamp potentials of 0 and −60 mV.

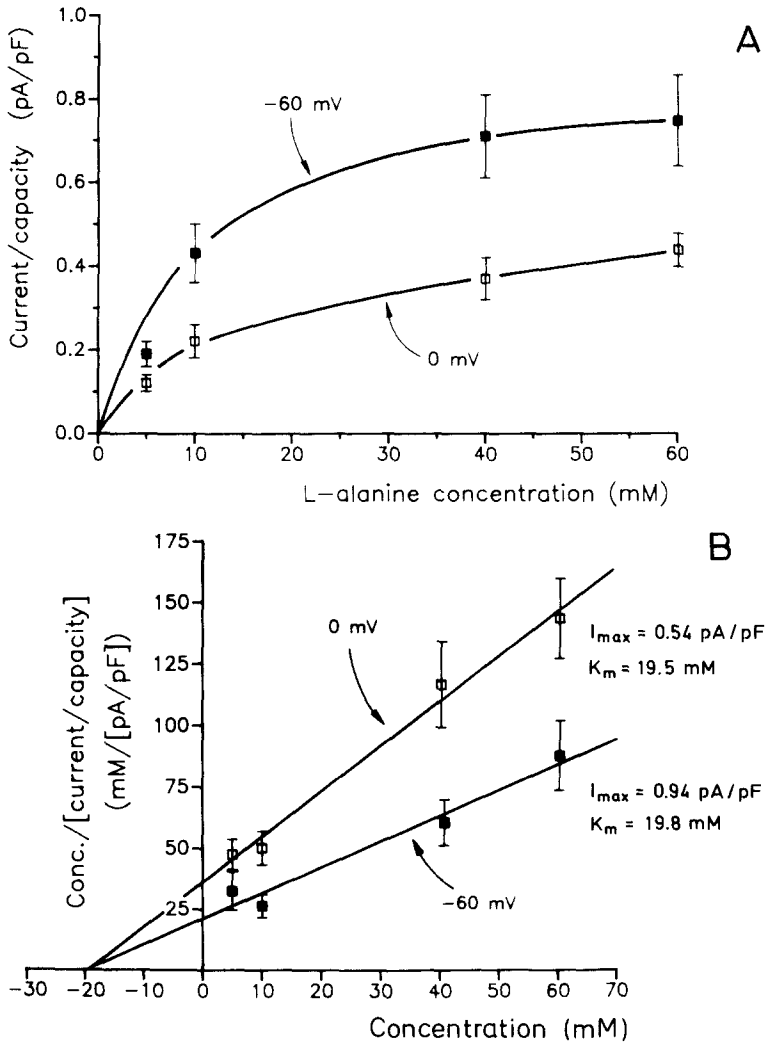

FIGURE 4. Dependence of L-alanine–driven, inward-directed sodium current on extracellular L-alanine concentration and transmembrane potential in the absence of a sodium gradient. (*A*) L-alanine–driven sodium current as a function of extracellular L-alanine concentration. Results from six experiments were standardized to the respective cell capacity and mean values ± SEM are presented. Curves were fitted by eye. Pipette solution: 140 mM Na-Cyclamate, 0.73 mM $CaCl_2$, 1 mM EGTA, 60 mM D-mannitol, pH 7.2. External solution: 140 mM Na-cyclamate, 1.3 mM $CaCl_2$, 0–60 mM D-mannitol, 0–60 mM L-alanine, pH 7.4. Cell capacity ranged from 3.6 to 12.6 pF. Currents measured at 0 and −60 mV are displayed. (*B*) In Hanes plots the data were fitted in linear form yielding the indicated kinetic parameters, apparent K_m ($-K_m = x$ axis intercept), and apparent I_{max} (1/slope).

hyperpolarization to −60 mV decreased the K_m value for sodium to 7.2 ± 2.1 mM and increased the I_{max} to 1.09 ± 0.08 pA/pF.

Coupling Stoichiometry

To obtain information on the stoichiometry of the cotransport, the experimental results from Fig. 7 were fitted to the Hill equation and a corresponding Hill plot is shown in Fig. 8. The resulting Hill coefficients are close to unity. Also, the cotransport current data measured as a function of extracellular L-alanine concentration (from Fig. 5) yield Hill coefficients close to unity, $n = 1.11$ at 0 mV and $n = 1.03$

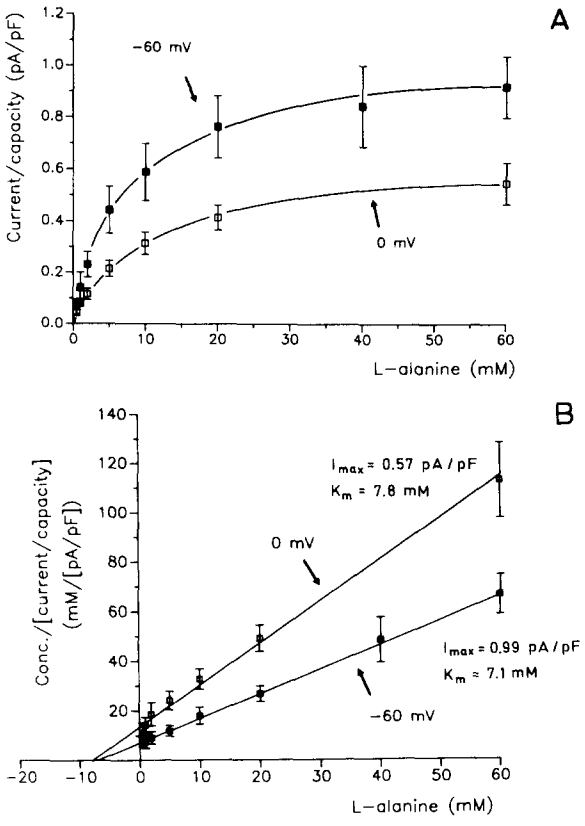

FIGURE 5. Dependence of L-alanine-driven, inward-directed sodium current on extracellular L-alanine concentration and transmembrane potential in the presence of a large sodium gradient. (*A*) L-alanine–driven sodium current as a function of extracellular L-alanine concentration. Results from four experiments were standardized to the respective cell capacity and mean values ± SEM are presented. Curves were fitted by eye. Pipette solution: 140 mM Tris-cyclamate, 0.73 mM $CaCl_2$, 1 mM EGTA, 40 mM D-mannitol, pH 7.2. External solution: 140 mM Na-cyclamate, 1.3 mM $CaCl_2$, 0–40 mM D-mannitol, 0–40 mM L-alanine, pH 7.4. Cell capacity ranged from 3.1 to 10.1 pF. Currents measured at 0 and −60 mV are displayed. (*B*) The L-alanine–sodium cotransport current data measured at 0 and −60 mV are rearranged in Hanes plots.

at −60 mV. These Hill coefficients suggest a sodium: L-alanine coupling stoichiometry of 1:1. The Hill coefficients were unchanged by cell hyperpolarization.

Phenylalanine-driven Sodium Current

The neutral amino acid phenylalanine had an effect on the whole-cell current similar to that of L-alanine. In Fig. 9*A* a typical experiment with increasing extracellular concentrations of L-phenylalanine is shown. The figure illustrates the concentration dependence of the phenylalanine-driven sodium current and also the saturation of the cotransporter current at high substrate concentrations. The data of four experi-

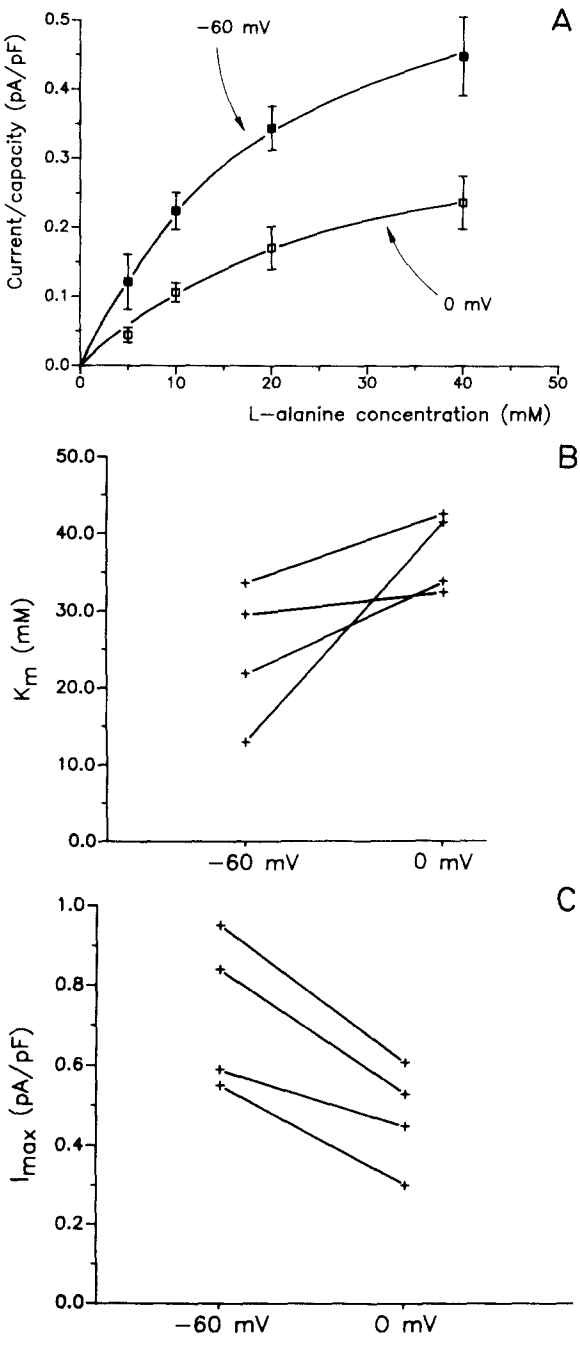

FIGURE 6. Dependence of L-alanine-driven, inward-directed sodium current on extracellular L-alanine concentration and transmembrane potential in the presence of a small sodium gradient. (*A*) L-alanine–driven sodium current as a function of extracellular L-alanine concentration. Results from four experiments were standardized to the respective cell capacity and mean values ± SEM are presented. Curves were fitted by eye. Pipette solution: 140 mM Tris-cyclamate, 0.73 mM $CaCl_2$, 1 mM EGTA, 40 mM D-mannitol, pH 7.2. External solution: 30 mM Na-cyclamate, 110 mM Tris-cyclamate, 1.3 mM $CaCl_2$, 0–40 mM D-mannitol, 0–40 mM L-alanine, pH 7.4. Cell capacity ranged from 4.8 to 6.5 pF. Currents measured at 0 and −60 mV are displayed. (*B*) Effect of transmembrane potential on K_m for alanine. Mean values: 37.6 ± 3.0 mM at 0 mV and 24.5 ± 5.3 mM at −60 mV clamp potential. (*C*) Effect of transmembrane potential on I_{max}. Mean values: 0.48 ± 0.08 pA/pF at 0 mV and 0.73 ± 0.11 pA/pF at −60 mV clamp potential.

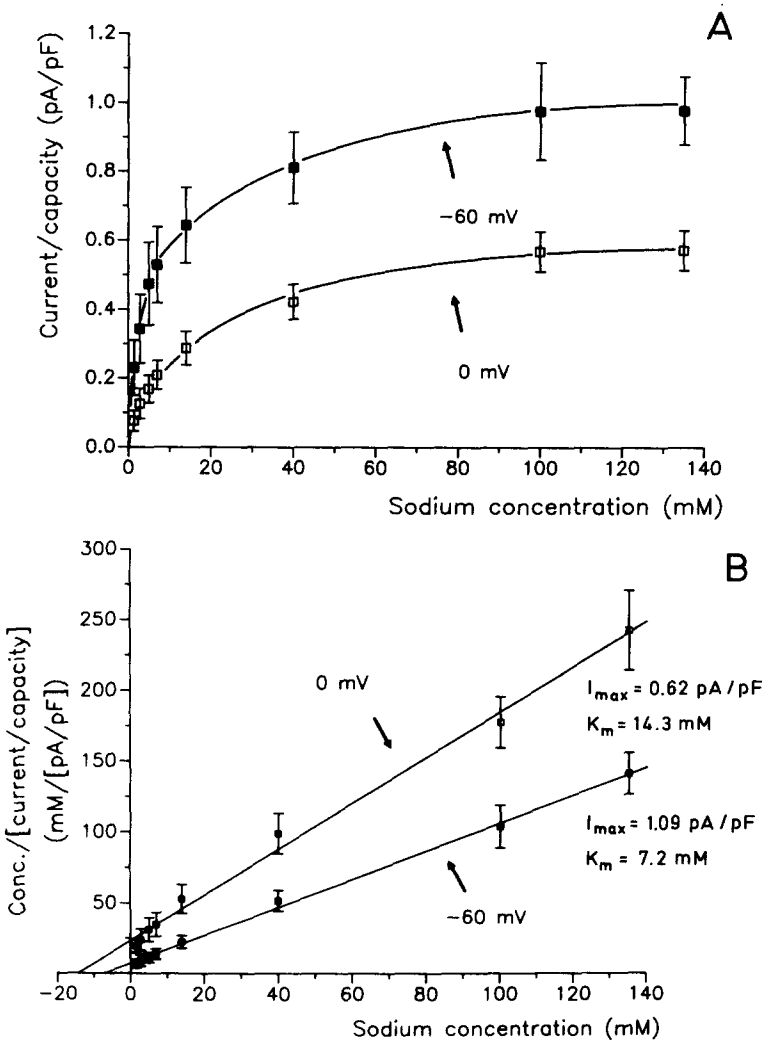

FIGURE 7. Dependence of L-alanine–driven, inward-directed sodium current on extracellular sodium concentration and transmembrane potential. (*A*) L-Alanine–driven sodium current as a function of extracellular sodium concentration. Results from four experiments were standardized to the respective cell capacity and mean values ± SEM are presented. Curves were fitted by eye. Pipette solution: 140 mM Tris-cyclamate, 0.73 mM $CaCl_2$, 1 mM EGTA, 60 mM D-mannitol, pH 7.2. External solution: 0–140 mM Na-cyclamate, 0–140 mM Tris-cyclamate, 1.3 mM $CaCl_2$, 60 mM D-mannitol, or 60 mM L-alanine, pH 7.4. Cell capacity ranged from 6.0 to 11.4 pF. Currents measured at 0 and −60 mV are displayed. (*B*) The data from *A* are illustrated as Hanes plots.

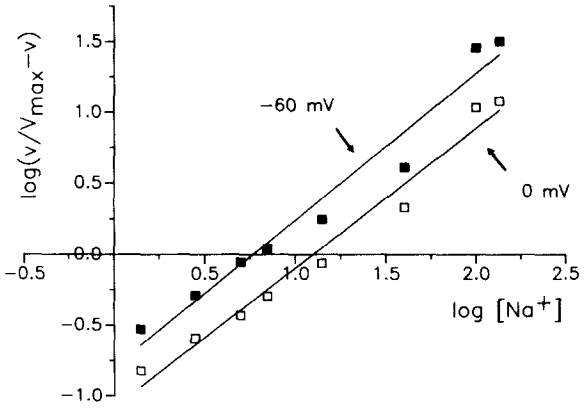

FIGURE 8. Hill plots of sodium–alanine cotransporter current data. Hill plots of data measured under zero-*trans* conditions and as a function of extracellular sodium concentration (shown in Fig. 7) reveal Hill coefficients close to 1 (n = 1.11 at 0 mV and n = 1.03 at −60 mV). Data points were fitted by linear regression.

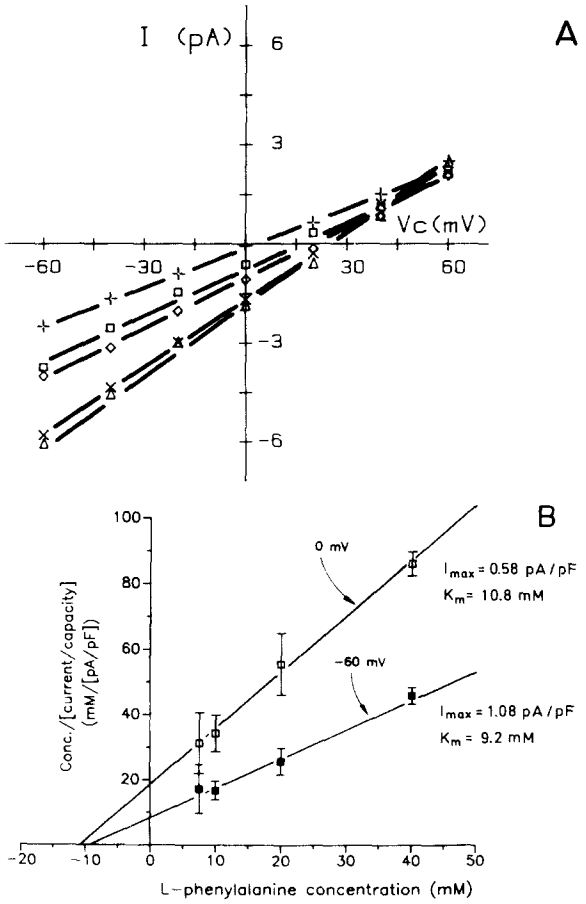

FIGURE 9. Phenylalanine-driven, inward-directed sodium current. (*A*) A typical experiment with varying extracellular phenylalanine concentrations: 0 (+), 5 (□), 7.5 (◇), 10 (×), and 20 mM (△). Pipette solution: 140 mM Na-cyclamate, 20 mM D-mannitol, 0.73 mM $CaCl_2$, 1 mM EGTA, pH 7.2. External solution: 140 mM Na-cyclamate, 1.3 mM $CaCl_2$, 0–20 mM D-mannitol, 0–20 mM L-phenylalanine, pH 7.4. Cell capacity was 5.7 pF. (*B*) The sodium–phenylalanine cotransport data from four experiments are presented in Hanes plots. Cell capacities ranged from 3.7 to 10.4 pF.

ments were standardized to cell capacity and mean current values are used in Hanes plots shown in Fig. 9 *B*. The kinetic parameters, calculated from the plot, revealed apparent maximal transport rates of I_{max} = 0.58 and 1.08 pA/pF for 0 mV and −60 mV clamp potential, respectively, and apparent K_m values of 10.8 and 9.2 mM L-phenylalanine, respectively.

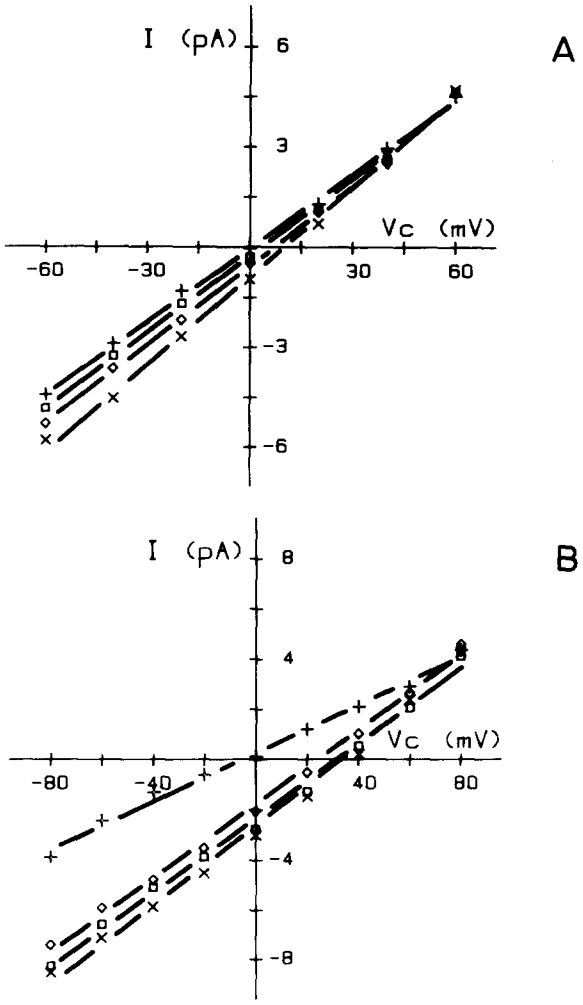

FIGURE 10. Simultaneous cotransport of L-alanine and L-phenylalanine. The figure shows data on the inward-directed sodium currents induced by L-alanine and L-phenylalanine alone or applied together. The symbols in *A* denote control (+), 5 mM L-alanine (□), 5 mM L-phenylalanine (◇), and 5 mM L-alanine + 5 mM L-phenylalanine (×). In B, higher substrate concentrations were used: control (+), 30 mM L-alanine (□), 30 mM L-phenylalanine (◇), and 30 mM L-alanine + 30 mM L-phenylalanine (×).

Furthermore, experiments were performed concerning a possible competition of L-alanine and L-phenylalanine for the cotransporter. Small concentrations of L-phenylalanine induced a similar sodium current as the same concentration of L-alanine. When the two amino acids were applied simultaneously, their effects were additive (Fig. 10 *A*). At higher amino acid concentrations (30 mM) there was no distinct additivity of the currents (Fig. 10 *B*). This suggests that the two amino acids compete for the same cotransport system.

DISCUSSION

Whole-cell measurements of the alanine-driven sodium current into isolated single cells does not distinguish between transport currents occuring across the apical or the basolateral cell membrane. Since the transport of L-alanine at the peritubular side has been shown to be independent of sodium and not electrogenic (Samarzija and Frömter, 1982; Silbernagl, 1988), it can be concluded that the sodium–alanine cotransport currents described in this study result from cotransport systems of the luminal cell membrane.

General Properties

Some basic characteristics of the electrogenic transport of neutral amino acids across the luminal membrane of proximal tubule cells like sodium dependence (Fox et al., 1964; Ullrich et al., 1974, 1976; Fass et al., 1977), stereospecificity (Fass et al., 1977; Silbernagl and Völkl, 1977), or saturation at high substrate concentrations (Ullrich et al., 1974, 1976; Evers et al., 1976; Fass et al., 1977) have been reproduced by us with the whole-cell recording technique. Also, in agreement with Samarzija and Frömter (1982), it was shown that L-alanine and L-phenylalanine are transported by the same cotransport system.

Coupling Stoichiometry

The experimental data on the cotransport current measured under zero-*trans* conditions suggest a sodium:alanine coupling stoichiometry of 1:1 (Fig. 8). However, from these data the existence two sodium binding sites with low cooperativity can not be excluded (Segel, 1975). The coupling stoichiometry was not affected by transmembrane potential. Studies with BBMV from rabbit proximal convoluted tubule (Kragh-Hansen et al., 1984) provided a coupling stoichiometry of 1:1 for the sodium–phenylalanine cotransport. A coupling stoichiometry of 1:1 was also derived for the A-system sodium–alanine cotransporter of pancreatic acinar cells (Jauch et al., 1986).

Transport Capacity

In the proximal convoluted tubule L-alanine is reabsorbed almost completely. In vivo micropuncture studies in rat proximal convoluted tubules showed that within the first 2 mm of the proximal tubule >90% of the filtered L-alanine is extracted from the tubule lumen (Silbernagl, 1981). The question arises whether the alanine-driven sodium current, recorded in the present study in single proximal tubule cells, can account for the alanine resorption observed in situ. Such an estimation requires us to make several assumptions. The number of cells in a proximal convoluted tubule 2 mm in length can be estimated to be ~2,000, assuming a cell diameter of ~10 μm (Kaissling and Kriz, 1979) and 10 cells surrounding the tubule lumen. In rabbits the plasma concentration of L-alanine and thus the concentration of the ultrafiltrate is ~500 μM (Block and Hubbard, 1962). The flow rate in the nephron is ~20 nl/min (Sonnenberg and Deetjen, 1964) or 0.33 nl/s. For a 90% resorption within the first 2 mm of the proximal convoluted tubule ~450 μM must be reabsorbed. Thus it can be estimated that on average each cell must reabsorb $7.43 \cdot 10^{-17}$ mol L-alanine/s,

corresponding to a current of 7.17 pA per cell at a sodium–alanine coupling ratio of 1:1.

From the Hanes plot in Fig. 5 *B*, derived from measurements at −60 mV cell potential and at room temperature (22–24°C), a current of 0.068 pA/pF is calculated for an extracellular alanine concentration of 500 μM. As the Q_{10} value was shown in this study to be 2.95 ± 0.29, the cotransporter current yields 0.29 pA/pF at 37°C. From the average capacity of 8.0 ± 1.1 pF per cell a mean current of 2.30 pA/cell results. This is about one-third of the current per cell derived from the above estimation. However, it must be taken into account that in isolated cells part of the brush border will be lost during the isolation procedure. In conclusion, the alanine-driven sodium current in single proximal tubule cells described in this study is in the same order of magnitude as that estimated for in situ conditions. Thus, the investigated cotransport system has the capacity to account for the resorption of the glomerularly filtered L-alanine in the proximal tubule.

The sodium–alanine cotransporter was previously investigated with the whole-cell recording technique in pancreatic acinar cells (Jauch and Läuger, 1986). An apparent I_{max} of 33 mA/m^2 cell membrane area was calculated. The correction of our data for 37°C and adjusted to m^2 membrane area, assuming that a specific membrane capacity of 1 μF/cm^2 yields for the apparent I_{max} a comparable value of 41.2 mA/m^2. Thus, the sodium–alanine cotransport systems in convoluted proximal tubule and pancreas acinus cells have similar transport capacities.

Kinetic Analysis

Kinetic data on sodium–alanine cotransport have been reported in studies using rabbit renal BBMV (Fass et al., 1977; Jorgenson and Sheikh, 1987; Lynch and McGivan, 1987). In these investigations the initial fluxes of radiolabeled alanine were usually measured in the absence of a membrane potential and after preincubation of vesicles in substrate-free medium, thus assuming zero-*trans* conditions for initial fluxes. K_m values for L-alanine of 400 μM (Fass et al., 1977) and 2.1 mM (Jorgenson and Sheikh, 1987) were calculated. A study using BBMV isolated from pig kidney revealed a K_m of 2.5 mM L-alanine (Lynch and McGivan, 1987). Therefore, the kinetic data concerning cotransporter affinity for alanine originating from BBMV studies vary over almost one order of magnitude. In vivo micropuncture studies in intact proximal convoluted tubules of rat kidney measuring the cell depolarization induced by the sodium–alanine cotransport revealed an apparent K_m of 6.6 mM L-alanine and a V_{max} of +32.4 mV (Samarzija and Frömter, 1982). Our experimental data, measured at a clamp potential of −60 mV and with an inward-directed sodium gradient, yielded an apparent K_m of 7.1 mM L-alanine (Fig. 5 *B*). Moreover, high substrate concentrations depolarized the cells by about +30 mV, measured under current clamp conditions. Therefore, our data are in good agreement with those reported from in vivo micropuncture experiments in rat kidney. The Michaelis-Menten kinetics of the cotransport current indicates that it originates from one cotransport system. However, this fact does not rule out the existence of several cotransport systems for alanine. The latter possibility seems unlikely since different cotransporters would then have the very same apparent affinity and potential dependence of the apparent K_m.

Fig. 7 shows that cotransport current depends on the driving force by the sodium gradient. Also, the effect of the sodium gradient on the transport kinetics can be deduced from Figs. 5 and 7. Whereas the apparent I_{max} was negligibly affected by the size of the sodium gradient at 0 mV, the apparent K_m for L-alanine was markedly increased by lowering the sodium gradient. This is in accordance with previous observations with renal BBMV, where a sodium gradient–dependent K_m and gradient-independent V_{max} for L-alanine (Fass et al., 1977) or L-phenylalanine were found (Evers et al., 1976).

Potential Dependence of Cotransport

In studies with BBMV it was shown that the cotransport of neutral amino acids and sodium depends on the transmembrane potential. The uptake of L-alanine Sigrist-Nelson, 1975; Fass et al., 1977) or L-phenylalanine (Evers et al., 1976) increased when the intravesicular space was rendered electrically negative by imposition of a K^+ diffusion potential in the presence of valinomycin.

The whole-cell recording technique allowed us to establish *I-V* curves, revealing an increase of the inward-directed cotransport currents with cell hyperpolarization, and a decrease of cotransport currents with depolarization. Especially at negative potentials, the *I-V* curves displayed no distinct deviation from linearity, whereas at increasing positive potentials the cotransport current diminished. This is in accordance with observations on the sodium–alanine cotransport system in pancreatic acinar cells (Jauch et al., 1986). For this system it was further shown, that the apparent K_m for sodium was influenced by the membrane potential (Jauch et al., 1986).

Before discussing the potential dependence of the cotransport in more detail, it is helpful to consider the transport mechanism by which the sodium–alanine cotransport occurs.

Simultaneous Transport Mechanism

The cotransport of sodium and alanine could occur by a simultaneous or consecutive (ping-pong) transport mechanism. A discrimination between these two possibilities is provided by the relationship between the K_m for alanine and the extracellular sodium concentration (Jauch and Läuger, 1986) as well as by the quotient of K_m/V_{max} (Segel, 1975; Kessler and Semenza, 1983). With a consecutive or ping-pong mechanism the K_m for alanine should decrease with decreasing extracellular sodium concentration and the quotient of K_m/I_{max} should be left unaltered. The comparison of results from experiments performed with different extracellular sodium concentration (Figs. 5 and 7) reveals an inverse relationship between the K_m for alanine and extracellular sodium concentration, as well as an increasing quotient K_m/I_{max}, excluding a consecutive transport mechanism and making a simultaneous transport mechanism likely (Segel, 1975; Kessler and Semenza, 1983; Jauch and Läuger, 1986).

The potential dependence of cotransporter kinetics can be explained by potential effects on the translocation step as well as on potential-dependent binding or unbinding of the sodium ion to or from the carrier complex (Hopfer and Groseclose, 1980; Restrepo and Kimmich, 1985; Sanders et al., 1984; Jauch and Läuger, 1985; Geck and Heinz, 1989).

Potential Dependence of Substrate Binding

A voltage-dependent binding or unbinding of sodium to or from the carrier complex can be explained by a model of an "ion-well' (Hopfer and Groseclose, 1980; Sanders et al., 1984) or a narrow access channel (so-called high-field access channel), through which sodium ions have to move in order to reach or leave the binding site (Jauch and Läuger, 1986; Läuger, 1987). Inside the access channel, part of the transmembrane potential will be sensed by the sodium ion, rendering its binding or unbinding potential dependent.

The potential dependence of the apparent K_m for sodium, observed in this study (Fig. 7 *B*) is an "obvious manifestation of a high-field access channel concept" as defined by Läuger and Jauch (1986). Indications for an ion-well (high-field access channel) concept have also been found for the sodium–sugar cotransporter (Hopfer and Groseclose, 1980; Restrepo and Kimmich, 1985; Kimmich and Randles, 1988) or for the A-system sodium–alanine cotransporter in pancreatic acinar cells (Jauch and Läuger, 1986).

The binding or unbinding of the electrically neutral substrate L-alanine can be assumed to be unaffected by the transmembrane potential (Läuger and Jauch, 1986). This is in agreement with our observation, where the apparent K_m for L-alanine was independent of the clamp potential (Fig. 5 *B*) at high extracellular sodium concentration (140 mM). Experiments performed with $[Na^+]_o$ = 30 mM revealed a potential dependence of the apparent K_m for alanine (Fig. 6). However, this sodium concentration is close to the K_m of the cotransporter for sodium, which is affected by the transmembrane potential (Fig. 7). Thus, the potential dependence of the K_m for alanine at low $[Na^+]_o$ can be explained by a potential-dependent binding or unbinding of sodium.

Potential Dependence of Translocation

Furthermore, the results of the present study revealed a potential dependence of the apparent I_{max}, measured as a function of extracellular sodium as well as of extracellular alanine. A potential-dependent sodium binding or unbinding can hardly be responsible for the potential dependence of I_{max} when the current was measured as a function of alanine, because in these experiments sodium was present in a concentration (140 mM) far above its apparent K_m (Fig. 7 *B*). This suggests that changes in I_{max} result from a voltage effect on the translocation step. A potential-dependent V_{max} was reported for the sodium–sugar cotransporter (Barbarat and Podevin, 1989). The existence of a potential effect on the maximal transport rate of cotransport systems has also been postulated in several theoretical treatments (Geck and Heinz, 1976; Turner, 1981; Sanders et al., 1984).

Conclusion

The kinetic analysis of the whole-cell current data obtained from the sodium–alanine cotransporter located in the BBM of proximal tubule cells (S1 segment) revealed mixed effects of transmembrane potential. First, we showed that transmembrane potential affects the binding or unbinding of sodium at the cotransporter binding

site, indicating a high-field access channel. Second, the potential dependence I_{max} suggests a potential effect on the translocation steps.

We are grateful to Prof. Dr. K. J. Ullrich for his great interest in this work and for his valuable discussion. We thank Prof. P. Läuger and Drs. G. Burckhardt and A. Schmid for manuscript reading and stimulating discussion. Furthermore, we thank W. Hampel and his workshop for most skillful development and preparation of technical devices.

J. Hoyer was supported by a grant (Ho-1103/1-1) from the Deutsche Forschungsgemeinschaft (DFG).

Original version received 27 December 1989 and accepted version received 26 November 1990.

REFERENCES

Barbarat, B., and R. A. Podevin. 1989. Membrane potential effects on Na^+-pantothenate and D-glucose co-transports across renal brush-border membrane vesicles. Proceedings of the International Union of Physiological Sciences. XVII. Helsinki. 374. (Abstr.)

Bezanilla, F. 1985. A high capacity data recording device based on a digital audio processor and a video cassette recorder. *Biophysical Journal.* 47:437–441.

Biagi, B., T. Kubota, M. Sohtell, and G. Giebisch. 1981. Intracellular potentials in rabbit proximal tubules perfused *in vitro*. *American Journal of Physiology.* 240:F200–F210.

Block, W. D., and R. W. Hubbard. 1962. Amino acid concentration of rabbit urine and plasma. *Archives of Biochemistry and Biophysics.* 96:557–661.

Burckhardt, G., R. Kinne, G. Stange, and H. Murer. 1980. The effects of potassium and membrane potential on sodium-dependent glutamic acid uptake. *Biochimica et Biophysica Acta.* 559:191–201.

Burg, M., C. Patlak, N. Green, and D. Villey. 1976. Organic solutes in fluid absorption by renal proximal convoluted tubules. *American Journal of Physiology.* 231:627–637.

Evers, J., H. Murer, and R. Kinne. 1976. Phenylalanine uptake in isolated renal brush border membrane vesicles. *Biochimica et Biophysica Acta.* 426:598–615.

Fass, S. J., M. R. Hammerman, and B. Sacktor. 1977. Transport of amino acids in renal brush border membrane vesicles. *Journal of Biological Chemistry.* 252:583–590.

Fox, M., S. Thier, E. Rosenberg, and S. Segal. 1964. Ionic requirements for amino acid transport in the rat kidney cortex slices. I. Influence of extracellular ions. *Biochimica et Biophysica Acta.* 79:167–176.

Frömter, E. 1981. Electrical aspects of tubular transport of organic substances. *In* Renal Transport of Organic Substances. R. Greger, F. Lang, and S. Silbernagl, editors. Springer Verlag GmbH, Berlin, Heidelberg, New York. 30–44.

Frömter, E. 1982. Electrophysiological analysis of rat renal sugar and amino acid transport. I. Basic phenomena. *Pflügers Archiv.* 393:179–189.

Geck, P., and E. Heinz. 1976. Coupling in secondary transport: effect of electrical potentials on the kinetics of ion linked co-transport. *Biochimica et Biophysica Acta.* 443:49–63.

Geck, H., and E. Heinz. 1989. Secondary active transport: introductory remarks. *Kidney International.* 36:334–341.

Gögelein, H., and R. Greger. 1987. Properties of single K^+ channels in the basolateral membrane of rabbit proximal straight tubules. *Pflügers Archiv.* 410:288–295.

Hamill, O. P., A. Marty, E. Neher, B. Sakmann, and F. J. Sigworth. 1981. Improved patch-clamp techniques for high resolution current recording from cells and cell-free membrane patches. *Pflügers Archiv.* 391:85–100.

Heidrich, H. G., and M. Dew. 1977. Homogeneous cell populations from rabbit kidney cortex. *Journal of Cell Biology.* 74:780–788.

Hopfer, U., and R. Groseclose. 1980. The mechanism of Na^+-dependent D-glucose transport. *Journal of Biological Chemistry.* 255:4453–4462.

Hoshi, T. 1976. Electrophysiological studies on amino acid transport across luminal membrane of proximal tubule cell of triturus kidney. *In* Amino Acid Transport and Uric Acid Transport. S. Silbernagl, F. Lang, and R. Greger, editors. G. Thieme Verlag, Stuttgart. 96–103.

Hoyer, J., and H. Gögelein. 1989. Whole-cell recording of sodium coupled transport of alanine or phenylalanine in single rabbit proximal tubule cells. *Biological Chemistry Hoppe-Seyler.* 370:623. (Abstr.)

Jauch, P., and P. Läuger. 1986. Electrogenic properties of the sodium-alanine cotransporter in pancreatic acinar cells. II. Comparison with transport models. *Journal of Membrane Biology.* 94:117–127.

Jauch, P., P. Läuger, and O. H. Peterson. 1986. Electrogenic properties of the sodium-alanine cotransporter in pancreatic acinar cells. I. Tight-seal whole-cell recordings. *Journal of Membrane Biology.* 94:99–115.

Jorgenson, K. E., and M. I. Sheikh. 1987. Renal transport of neutral amino acids. *Biochemical Journal.* 248:533–538.

Kaissling, B., and W. Kriz. 1979. Structural analysis of the rabbit kidney. *Advances in Anatomy Embryology and Cell Biology.* 56:21–25.

Kessler, M., and G. Semenza. 1983. The small-intestinal Na^+, D-glucose cotransporter: an assymmetric gated channel (or pore) responsive to $\gamma\chi$. *Journal of Membrane Biology.* 76:27–56.

Kimmich, G. A., and J. Randles. 1988. Na^+-coupled sugar transport: membrane potential-dependent K_m and K_i for Na^+ . *American Journal of Physiology.* 255:C486–C494.

Kragh-Hansen, U., H. Roigaard-Petersen, C. Jacobsen, and M. I. Sheikh. 1984. Renal transport of neutral amino acids: tubular localization of Na^+-dependent phenylalanine- and glucose-transport systems. *Biochemical Journal.* 220:15–24.

Lapointe, J. P., R. Laprade, and J. Cardinal. 1984. Transepithelial and cell membrane electrical resistances of the rabbit proximal convoluted tubule. *American Journal of Physiology.* 247:F637–F649.

Läuger, P. 1987. Dynamics of ion transport systems in membranes. *Physiological Reviews.* 67:1296–1331.

Läuger, P., and P. Jauch. 1986. Microscopic description of voltage effects on ion-driven cotransport systems. *Journal of Membrane Biology.* 91:275–284.

Lingard, J. M., G. Rumrich, and J. A. Young. 1973. Kinetics of L-histidine transport in the proximal convolution of the rat nephron studied using the stationary microperfusion technique. *Pflügers Archiv.* 342:13–28.

Lynch, A. M., and J. D. McGivan. 1987. Evidence for a single common Na^+-dependent transport system for alanine, glutamine, leucine and phenylalanine in brush-border membrane vesicles from bovine kidney. *Biochimica et Biophysica Acta.* 899:176–184.

Marty, A., and E. Neher. 1983. Tight-seal whole-cell recording. *In* Single Channel Recording. B. Sakmann, and E. Neher, editors. Plenum Publishing Corp., New York. 107–122.

Mircheff, A. K., I. Kippen, B. Hirayama, and E. M. Wright. 1982. Delineation of sodium-stimulated amino acid transport pathways in rabbit kidney brush border vesicles. *Journal of Membrane Biology.* 64:113–122.

Poujeol, P., and A. Vandewalle. 1985. Phosphate uptake by proximal cells isolated from rabbit kidney: role of dexamethasone. *American Journal of Physiology.* 249:F74–F83.

Restrepo, D., and G. A. Kimmich. 1985. The mechanistic nature of the membrane potential dependence of sodium-sugar transport in small intestine. *Journal of Membrane Biology.* 87:159–172.

Rohlicek, V., U. Fröbe, H. Gögelein, and R. Greger. 1989. Versatile supplement device with remote control for the control of patch clamp experiments. *Pflügers Archiv.* 413:444–446.

Samarzija, I., and E. Frömter. 1975. Electrical studies on amino acid transport across brushborder membrane of rat proximal tubule *in vivo*. *Pflügers Archiv.* 359:R119. (Abstr.)

Samarzija, I., and E. Frömter. 1982. Electrophysiological analysis of rat renal sugar and amino acid transport. III. Neutral amino acids. *Pflügers Archiv.* 393:199–209.

Sanders, D., U.-P. Hansen, D. Gradmann, and C. L. Slayman. 1984. Generalized kinetic analysis of ion-driven cotransport systems: a unified interpretation of ionic effects on Michaelis parameters. *Journal of Membrane Biology.* 77:123–152.

Schafer, J. A., and J. C. Williams. 1985. Transport of metabolic substrates by the proximal nephron. *Annual Review of Physiology.* 47:103–125.

Schwegler, J. S., A. Heuner, and S. Silbernagl. 1989. Electrogenic transport of neutral and dibasic amino acids in a cultured oppossum kidney cell line (OK). *Pflügers Archiv.* 414:543–550.

Segel, I. H. 1975. Enzyme Kinetics. J. Wiley & Sons, Inc., New York.

Sigrist-Nelson, K., H. Murer, and U. Hopfer. 1975. Active alanine transport in isolated brush border membranes. *Journal of Biological Chemistry.* 250:5674–5680.

Silbernagl, S. 1981. Renal transport of amino acids and oligopeptides. *In* Renal Transport of Organic Substances. R. Greger, F. Lang, and S. Silbernagl, editors. Springer Verlag, Berlin, Heidelberg, New York. 93–117.

Silbernagl, S. 1988. The renal handling of amino acids and oligopeptides. *Physiological Reviews.* 68:911–1007.

Silbernagl, S., and H. Völkl. 1977. Amino acid resorption in proximal tubule of rat kidney: stereospecificity and passive diffusion studied by continuous microperfusion. *Pflügers Archiv.* 367:221–227.

Sonnenberg, H., and P. Deetjen. 1964. Methode zur Durchströmung einzelner Nephronabschnitte. *Pflügers Archiv für die gesamte Physiologie.* 278:669–674.

Turner, R. J. 1981. Kinetic analysis of a family of cotransport models. *Biochemica et Biophysica Acta.* 649:269–280.

Ullrich, K. J. 1976. Renal tubular mechanisms of organic solute transport. *Kidney International.* 9:134–148.

Ullrich, K. J. 1979. Sugar, amino acid and Na^+ cotransport in the proximal tubule. *Annual Review of Physiology.* 41:181–195.

Ullrich, K. J., E. Frömter, I. Samarzija, J. Evers, and R. Kinne. 1976. Sodium dependence of amino acid transport in the proximal convolution of the rat kidney. *In* Amino Acid Transport and Uric Acid Transport. Symposium Innsbruck. S. Silbernagl, F. Lang, and R. Greger, editors. G. Thieme-Verlag, Stuttgart. 70–78.

Ullrich, K. J., G. Rumrich, and S. Klöss. 1974. Sodium dependence of the amino acid transport in the proximal convolution of the rat kidney. *Pflügers Archiv.* 351:49–60.